Heat partition in edge trimming of glass fiber reinforced polymer (GFRP) composites

Sheikh-Ahmad, Jamal ; Almaskari, Fahad; Hafeez, Farrukh

DOI:
10.1016/j.procir.2019.09.048

Document Version
Publisher's PDF, also known as Version of record

Citation for published version (Harvard):
Sheikh-Ahmad, J, Almaskari, F & Hafeez, F 2019, 'Heat partition in edge trimming of glass fiber reinforced polymer (GFRP) composites', *Procedia CIRP*, vol. 85, pp. 20-25. https://doi.org/10.1016/j.procir.2019.09.048

Available online at www.sciencedirect.com

ScienceDirect

Procedia CIRP 85 (2019) 20–25

www.elsevier.com/locate/procedia

2nd CIRP Conference on Composite Material Parts Manufacturing (CIRP-CCMPM 2019)

Heat partition in edge trimming of glass fiber reinforced polymer (GFRP) composites

Jamal Sheikh-Ahmad[a], Fahad Almaskari[b,]*, Farrukh Hafeez[c]

[a]*Department of Mechanical Engineering, Khalifa University of Science and Technology, SAN Campus, Abu Dhabi, United Arab Emirates*
[b]*Department of Aerospace Engineering, Khalifa University of Science and Technology, Main Campus, Abu Dhabi, United Arab Emirates*
[c]*University of Birmingham Dubai, Block 2, DIAC, Dubai, 341799, United Arab Emirates*

* Corresponding author. Tel.: +971-2-607-5577; fax: +971-2-447-2442. *E-mail address:* fahad.almaskari@ku.ac.ae

Abstract

Thermal loading of fiber reinforced composites during traditional machining is inevitable. This is due to the fact that most of the mechanical energy utilized in material removal is converted into heat, which is subsequently dissipated into the workpiece, the cutter and is carried away by the chips. Heat conduction into the workpiece might cause thermal damage if the generated temperatures exceeded the glass transition temperature of the epoxy matrix. In this work, the amount of heat flux applied to the machined edge and the temperature distribution in a multidirectional GFRP composite laminate was determined using an inverse heat conduction method. The spindle electric power, cutting forces and boundary temperatures on the workpiece were measured during edge trimming of the GFRP laminate with a PCD cutter at different spindle and feed speeds. The transient heat conduction problem in the laminate was simulated using the finite element method and the amount of heat flux conducted through the machined surface was determined. It was found that the heat flux conducted to the workpiece represented only a small fraction of the total heat and is more influenced by the feed speed than the spindle speed. The temperature of the machined surface was found to be lower than the glass transition temperature of epoxy for all cutting conditions tried in this study.

Peer-review under responsibility of the scientific committee of the 2nd CIRP Conference on Composite Material Parts Manufacturing.

Keywords: Edge trimming; GFRP; Resultant force RMS; Heat partition; Temperature distribution.

1. Introduction

Edge trimming is a necessary step in the process of composites parts manufacturing. Almost all composite parts require trimming after demolding to obtain the desired shape, dimensions and dimensional tolerances. It is widely accepted that the mechanical energy consumed in the trimming process is converted into heat, part of which is conducted to the composite part causing its temperature to rise. Exposure to high temperatures might cause irreversible thermodynamic change resulting in physical or chemical change in the composite, which might lead to adverse effects on the mechanical properties of the machined part through the introduction of thermal damage [1,4]. Heat is also a driving force for various tool wear mechanisms [5].

Current understanding of the heat partition in machining fibrous composites is not as well established as in conventional metallic materials. Most of the researchers in this area focused on the experimental measurement of temperature fields in the workpiece or cutting tool during the machining operation. Several researchers used various techniques to measure cutting temperatures and their effect on the quality of the composite part [3,6-9]. It was established in some of these works that the temperature on the machined surface exceeded the glass transition temperature of the epoxy resin. However, others indicated that the resin was not damaged (degraded) even at high cutting speeds [9].

Only a few attempts were made to investigate the heat partition problem in composites machining. Liu et al. [10] established the heat partition into the workpiece for helical milling of CFRP using the Conjugate Gradient Method. It was

Peer-review under responsibility of the scientific committee of the 2nd CIRP Conference on Composite Material Parts Manufacturing.
10.1016/j.procir.2019.09.048

concluded that 21% and 18.6% of the heat is evacuated through the workpiece during milling and drilling operations, respectively. More recently, Sheikh-Ahmad, et al. [11] carried out more comprehensive work to estimate the heat partition in edge trimming operation of CFRP using the inverse heat conduction technique. The heat partition ratios into the workpiece, tool and chips were found to be 0.07, 0.56 and 0.37, respectively.

Nomenclature

A_w	Projected contact area between cutter and workpiece
N	Spindle speed
P_e	Spindle electric motor power
P_m	Machining power
$\dot{Q}$	Total heat from thermal energy
$\dot{Q}_c$	Portion of heat carried by the chips
$\dot{Q}_e$	Portion of heat dissipated to the environment
$\dot{Q}_t$	Portion of heat conducted by the cutting tool
$\dot{Q}_w$	Portion of heat conducted to the workpiece
R_w	Heat partition ratio to the workpiece
SSE	Sum of the squares of error
T	Temperature of the GFRP laminate
T_∞	Ambient temperature
v_f	Feed speed
Y_i	Measured temperature history at location i
Y_j	Measured peak temperature at location j
c	Specific heat of GFRP laminate
f_z	Chip per tooth
h	Heat transfer coefficient (convection)
$k_{x,y,z}$	Heat conduction of the GFRP laminate in orthotropic directions
$\dot{q}_w$	Moving heat flux applied to the workpiece
t	Time
α	Conversion efficiency of mechanical energy to thermal energy
ε	Electric motor efficiency
ρ	Density of GFRP laminate

Most of the studies discussed above were conducted on CFRPs with little or no attention to composite parts made from other common reinforcements, such as GFRP. Furthermore, similar studies on GFRP were focused on measurement of cutting temperatures and limited type of machining operations, primarily drilling and milling. Woo et al. [12] established a relationship between the cutting temperature and damage during drilling and milling operations of woven GFRP. The authors concluded that higher feed rates generated lower cutting temperatures. Mkaddem et al. [13] predicted the temperature field in the workpiece subjected to milling operation with the finite element model. The authors represented the cutter as a moving heat source along the edge of the GFRP workpiece and assumed a Gaussian distribution of heat imparted to the workpiece on the trimmed surface. The authors successfully showed that the temperature distribution in the workpiece could be obtained with a moving heat source assumption for edge trimming operation.

This current study is an attempt to address the heat partition problem in a glass reinforced epoxy composite subjected to trimming operation. The amount of heat evacuated through the workpiece was estimated using an inverse heat conduction method. The transient and direction dependent heat condition problem in the workpiece was modeled using finite element method. A uniform moving heat source was applied to the workpiece in order to represent the energy source from machining. Boundary temperatures on the workpiece surface were measured with embedded thermocouples. The difference between the measured and simulated boundary temperatures was expressed in terms of objective functions which minimization allowed the estimation of the heat flux conducted to the workpiece.

2. Energy Conversion

It is widely accepted that most of the mechanical power spent in machining, P_m is converted into heat, which is then partitioned by conduction, convection and radiation into four regions, namely the workpiece ($\dot{Q}_w$), cutter ($\dot{Q}_t$), chips ($\dot{Q}_c$) and the environment ($\dot{Q}_e$). The energy partition equation in machining is expressed as,

$$P_m = \alpha\dot{Q} = \dot{Q}_w + \dot{Q}_t + \dot{Q}_c + \dot{Q}_e \qquad (1)$$

where α represents the efficiency of conversion from mechanical to thermal energy, which is assumed to be 95%. It is noted here that this is a rather conservative conversion coefficient inherited from the well-established theory of metal machining [14]. No such coefficient is yet established for machining fiber reinforced polymers, and the use of this value is considered a good first approximation. The mechanical power, P_m can be determined by directly measuring the spindle torque and rotation speed, or indirectly by measuring the spindle electric power, P_e using the expression,

$$P_m = \varepsilon P_{el} \qquad (2)$$

where ε is the efficiency of spindle electric motor.

3. Inverse Heat Conduction Method

Inverse heat conduction methods can be used to determine heat flux and temperatures on an inaccessible surface by measuring the temperatures on a remote accessible boundary [15]. This technique has been used by different authors to solve the heat partition problem in metal machining and grinding [16-18]. To provide a robust solution, boundary temperature measurements must be spread apart in order to capture the spatial characteristics of the temperature distribution in the object.

Fig.2 shows the heat transfer model used to simulate edge milling of GFRP laminate. The heat diffusion problem in the workpiece is 3-D nonlinear and transient as represented by the heat conduction equation without internal heat generation:

$$\frac{\partial}{\partial x}\left(k_x\frac{\partial T}{\partial x}\right) + \frac{\partial}{\partial y}\left(k_y\frac{\partial T}{\partial y}\right) + \frac{\partial}{\partial z}\left(k_z\frac{\partial T}{\partial z}\right) = \rho c\frac{\partial T}{\partial t} \qquad (3)$$

The internal heat generation term was removed from the general heat conduction equation and the heat from machining

was treated as moving boundary condition, as explained below. This provides a true representation of the physical problem. The boundary conditions applied to the laminate are as follows:

- Heat is lost by convection on the top, bottom and machined surfaces, using h_1 and h_2 on the respected surfaces as indicated on the figure, where η is normal to the surface,

$$-k_\eta(T)\frac{\partial T}{\partial \eta} = h(T - T_\infty) \qquad (4)$$

- A moving uniform heat source of magnitude $\dot{q}_w$ represents the heat flux conducted into the workpiece through the machined surface,

$$-k_x(T)\frac{\partial T}{\partial x}(x,y,z,t) = \dot{q}_w \qquad (5)$$

- The remaining surfaces are assumed to be insulated and the problem is subjected to the initial condition $T(x,y,z,t) = T_o$ at t = 0, where t is time.

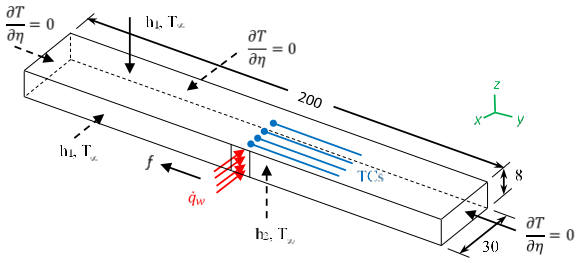

Fig. 1. Model used for simulation of heat conduction in the workpiece. TCs represent the location of thermocouples used for boundary temperature measurement.

The heat transfer coefficient on the machined surface and the top surface were set higher than the bottom surface (h_1>h_2) because these two surfaces were subjected to more air movement due to the suction from the dust collector and the rotating tool. The heat transfer coefficients used in the current simulation were h_1 = 100 W/°K.m^2 and h_2 = 50 W/°K.m^2. It is worth noting here that the value of h did not greatly affect the overall solution of the problem. This observation was also reported by [16]. The GFRP laminate is assumed to be quasi-isotropic and its bulk thermal properties are directional and temperature dependent. Exact values of the bulk thermal properties of the GFRP used in the present study were not available. Instead, the values for a similar laminate were obtained from [17] and are shown in Table (1).

Table 1. Bulk thermal properties of quasi-isotropic GFRP laminate [17]

Property	Units	T=300 °K	T=423 °K
ρ	g/cm^3	1.570	1.570
k_x, k_y	W/m-°K	0.89	0.89
k_z	W/m-°K	0.39	0.39
c	J/g-°K	0.8882	1.301

The moving heat flux was assumed to be uniformly distributed over the projected area of contact between the cutter and the workpiece, which is 5mm wide and 8mm high. The exact area of contact is actually cylindrical (quarter of a cylinder). However, the projected area was used in the present analysis for simplicity. During model development, linear heat flux distribution was also tried and found to have negligible effect on the results. Similar findings were also reported by [16]. DFLUX user subroutine was utilized to introduce the moving heat flux in the numerical simulation. The magnitude of heat flux was determined by minimizing the objective functions in equations (6) and (7) over time and space domains, respectively:

$$SSE1 = \sum_{i=1}^{n}\sum_{t=1}^{m}(Y_i(t) - T_i(t))^2 \qquad (6)$$

$$SSE2 = \sum_{j=1}^{l}\sum_{x=1}^{k}\left(Y_j(x) - T_j(x)\right)^2 \qquad (7)$$

where Y_i is measured temperature history and T_i is simulation temperature history for thermocouple location i and Y_j is the measured peak temperature and T_j is the simulated peak temperature at location x for thermocouple location j.

Numerical model for the workpiece was developed in Abaqus/Explicit. The element type used for the workpiece was DC3D8 (thermal analysis), a 3D 8-noded linear heat transfer brick type element, and 60000 elements and 68541 nodes were used. Fine mesh with element size 0.25x1x1mm^3 was used in the steep thermal gradient region and a coarse mesh of size 2.5x1x1mm^3 was used for the remaining regions. This mesh size was verified to provide a reasonable compromise between numerical convergence and computational time. Convergence of the solution of an explicit problem also relies on the time increment. This convergence was examined by adjusting the time increment implemented in Abaqus solver. It is was determined that a time increments of 0.01 second guaranteed a converging solution with adequate accuracy [11].

4. Experimental Methods

Edge trimming experiments were conducted on a 3-axis CNC router to generate cutting data for validating the numerical model. Fig. 2 shows photo of the experimental setup where a 500 mm long, 8 mm thick GFRP laminate was clamped to the machine table so that the long side can be trimmed along the edge in a climb cutting configuration. The GFRP laminate was fabricated by hand layup of plain-weave E-glass prepreg with the fiber orientation [0/90°], vacuum bagged and then autoclave cured. The fiber volume fraction was approximately 40%. The spindle speed and feed speed utilized were varied according to the parameters shown in Table 2, while the radial depth of cut was kept constant at 5mm. The cutter used was a 2-flute PCD milling tool with 10mm diameter, 100 mm total length and 12 mm flute length. The rake and clearance angles of the cutting edge were 0 and 15°, respectively, and the initial nose radius was 12 μm. Electric power required for machining was measured by a Load Control fast response power meter wired in line with the spindle motor. The net electric cutting power was calculated as the difference between the average spindle power during cutting and idling. The sampling rate for the power signal was 5kHz. The noise to signal ratio during cutting was in the order of 0.15. Measurements of boundary

temperatures were made by thermocouples mounted on the top surface of the laminate, approximately halfway as shown in Fig. 2. This allowed for the temperatures to reach steady state by the time the cutter passed by the thermocouples. Thermocouple beads were placed in 1.0 mm diameter, 1.5 mm deep holes drilled on the top surface at specific locations from the machined edge. The holes were filled with thermal conductive paste before inserting the thermocouple wires and the holes with beads in them were covered by adhesive tape to protect them from being sucked by the dust collection port. Gage 36, type K sheathed thermocouples were used in the experiment. The sampling rate for the thermocouples signals was 2Hz.

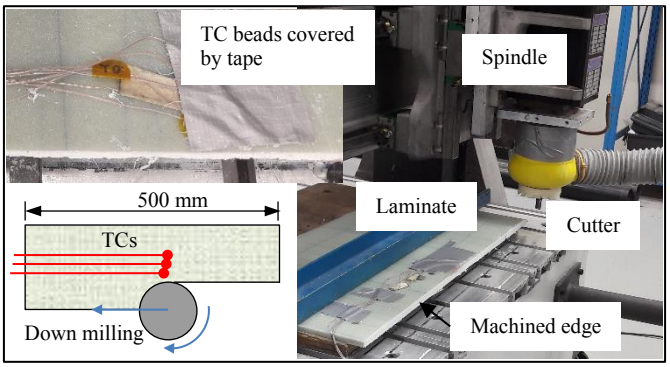

Fig. 2. Setup for edge milling experiments.

Table 2. Experimental conditions

Parameter	Values
Spindle speed, rpm	4000, 8000
Feed speed, mm/min	400, 800
Feed per tooth (mm/z)	0.025, 0.05, 0.10

5. Results and Discussion

5.1. Boundary temperatures

Figure 3 shows the temperature history for the surface mounted thermocouples when cutting with spindle speed of 8000 rpm and feed speed of 800 mm/min. Similar histories were obtained for the other cutting conditions. The temperature at each location rises rapidly as the tool passes by and then decreases slowly due to cooling. The peak temperature for each location is closely related to its distance perpendicular to the machined surface. The peak temperatures are also not aligned due to lags in heat conduction and due to misalignment of the holes drilled for the thermocouples. It is noted that once steady state is reached, these characteristic temperature histories exhibit the same behavior at different locations on the laminate surface which are at similar perpendicular distances from the machined surface. Figure 4 shows the measured peak temperatures for two repeats at the same cutting condition as a function of the perpendicular distance from the machined edge. It can be seen that the two repeats of the experiment produce similar temperatures and that the temperature gradient perpendicular to the machined edge follows a 3-parameter lognormal distribution function [11].

5.2. Determination of heat flux into the workpiece

Figure 4 shows the simulated peak temperatures along a line perpendicular to the machined surface for different values of heat flux $\dot{q}_w$ as indicated in the figure caption for the cutting condition 8000 rpm and 800 mm/min. It is evident that the simulated temperature gradients accurately capture the experimental trend with some variations in magnitude according to the value of the applied heat flux. The exact amount of $\dot{q}_w$ for the best match between experimental and simulated histories for this cutting condition was determined by minimizing the objective functions in Eqs. (6) and (7) while the heat flux magnitude was varied systematically. It was found that a minimum difference between the simulated and experimental temperature gradients is obtained when $\dot{q}_w = 237.5$ mJ/mm^2.s. The sum of the squares of the differences in this case was 54 $^oC^2$, as evaluated by Eq. (7). Table 3 shows the resulting heat flux applied at each cutting condition for obtaining minimum values of the objective functions as discussed above. The confidence intervals shown in the table represent the range of the heat flux results (or standard deviation, when applicable) obtained for each condition from the two experiment repeats and two optimization functions.

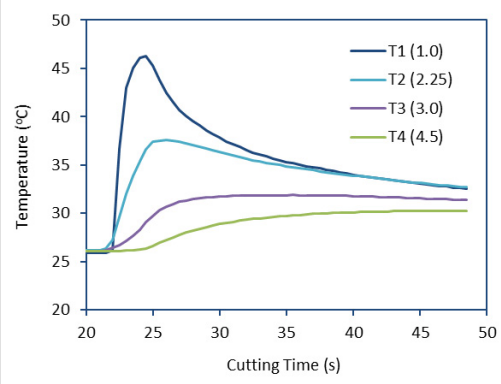

Fig. 3. Temperature history for the combination 8000 rpm, 800 mm/min. Numbers in parentheses show TC location from the machined edge.

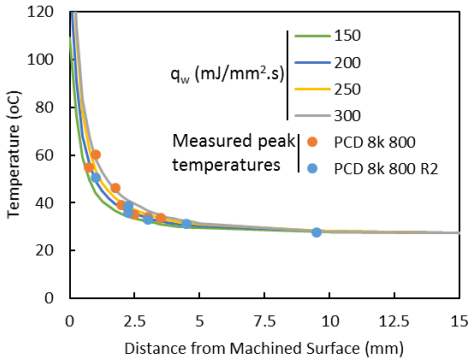

Fig. 4. Comparison between measured and simulated peak temperatures at different distances from the machined edge. The correct flux is 237.5 mJ/mm^2.s

The portion of the total heat conducted to the workpiece is determined by multiplying the heat flux by the projected contact area,

$$\dot{Q}_w = \dot{q}_w \cdot A_w \qquad (8)$$

Finally, the energy partition ratio, R_w is determined by dividing the portion of heat conducted to the workpiece by the total power,

$$R_w = \frac{\dot{Q}_w}{\varepsilon P_{el}} \qquad (9)$$

The spindle electric motor efficiency, ε was assumed to be 80%.

Table 3. Minimum values of heat flux applied to the machined surface for each cutting condition.

N (rpm)	v_f (mm/min)	f_z (mm)	$\dot{q}_w$ (mJ/mm^2.s)
8000.0	400.0	0.025	200.0±20.9
8000.0	800.0	0.05	237.5±34.2
4000.0	800.0	0.1	166.7±58.5

Table 4 lists the energy partition to the workpiece for the different cutting conditions used in this study. The confidence intervals shown for the electric power represent the range of the experimental data. The confidence levels for Q_w and R_w represent the uncertainty in these calculated quantities according to the analysis shown in Appendix A. It can be seen that only a small fraction of the total heat is conducted to the workpiece (3 to 7%). This is mainly due to the poor thermal conductivity of the GFRP material and the excellent conductivity of the PCD tool, which allows most of the heat to be channeled away by the cutter [11]. As shown in Fig. 5, the heat partition R_w decreases with an increase in the feed per tooth, with the highest value occurring at the smallest feed per tooth (i.e. smaller feed speed and higher spindle speed). Furthermore, the effect of feed speed on R_w is more profound than the effect of the spindle speed. This attributed to two reasons. First, lower feed speeds allow more time for heat to be conducted into the workpiece. Second, larger feed per tooth allows for more heat to be carried away by the chips, thus reducing the heat load on the workpiece. Compared to CFRP edge trimming, the heat partition to the workpiece was found to be 7% at a spindle speed of 8000 rpm and feed speed of 500 mm/min [11]. Compared to similar material removal processes in metals, we find that the heat partition into GFRP and CFRP is very small. [18] determined the heat partition into the workpiece in the dry milling of steel to vary with undeformed chip thickness from 10% to 50%. [19] determined this partition in face milling of 4340 steel to be 35%. Both of these works utilized an inverse heat conduction method to determine the heat partition.

Table 4. Energy partition into the workpiece for the different experiments

N (rpm)	v_f (mm/min)	f_z (mm)	P_{el} (W)	$\dot{Q}_w$ (W)	R_w
8000	400	0.025	184.5±5.04	8.3±0.0	0.07±0.007
8000	800	0.05	324.7±1.78	9.6±1.0	0.04±0.006
4000	800	0.1	311.4±3.72	6.9±2.1	0.03±0.010

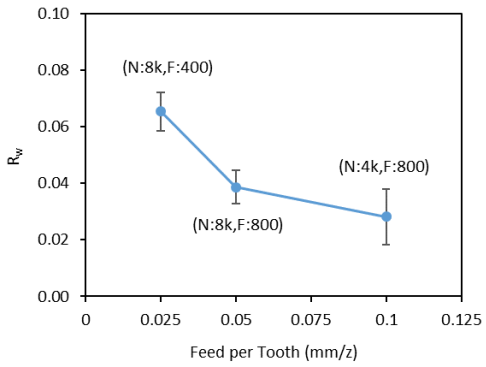

Fig. 5. Variation of the heat partition ratio R_w with cutting conditions.

5.3. Estimation of machined surface temperature

Fig. 6 shows the temperature distribution in the GFRP laminate when cutting at 8000 rpm and 800 mm/min. This temperature distribution was obtained by applying the estimated heat flux to the workpiece as described in section 5.2 (i.e. 237 mJ/mm^2.s). It can be seen that the heat penetration in the workpiece is very shallow due to the low thermal conductivity of GFRP. At the cutting zone, the maximum temperature occurs in the region of application of the heat flux just behind the center of the cutter. The maximum machined surface temperature was found to be 178 °C. Furthermore, it was found that the machined surface temperature decreased linearly with the feed per tooth. For all cutting conditions, the estimated maximum temperatures were below the glass transition temperature of the epoxy. Due to these relatively low temperatures and the short exposure time, thermal machining damage is not expected for the machining conditions used in this study [20].

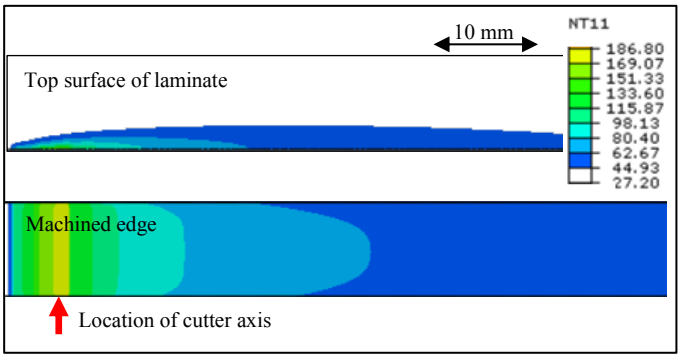

Fig. 6. Contours of the temperatures in the machined workpiece for edge trimming at 8000 rpm and 800 mm/min.

6. Conclusions

An inverse heat conduction method was used to determine the heat partition and temperature distribution in edge trimming of GFRP with a PCD cutter. A three dimensional numerical heat conduction model was used to represent the workpiece and the heat flux applied was estimated by minimizing the difference between measured and calculated boundary temperatures. Conclusions drawn from this work are:

1. Inverse heat conduction method is an effective and efficient technique for determining the heat partition in machining GFRP.
2. The portion of heat conducted to the GFRP workpiece was very small and varied with feed per tooth from 3% to 7%.
3. The portion of heat conducted to the workpiece was more sensitive to changes in the feed speed than changes in spindle speed.
4. The temperature of the machined surface was estimated to be below the glass transition temperature for all conditions used in the study.

Appendix A. Uncertainty Analysis

This appendix discusses uncertainties in the results due to experimental errors and uncertainties in thermal properties. The calculations of uncertainties were performed according to the analysis presented in [21].

For estimating uncertainty in the heat flux, a close form solution of the heat conduction equation (3) is required. However, such a solution is not available. Alternatively, we can get an idea about the uncertainty in the solution by solving the simple one dimensional heat conduction problem. This estimation of error might be valid to some extent because the material is isotropic in the xy plane and the measurement of boundary temperatures is performed in this plane perpendicular to the machined edge. So, at any given instant, the heat conduction problem could be viewed as being one dimensional.

The governing equation for one-dimensional steady state heat conduction is given by:

$$q_w = -k\partial T/\partial x = -k\,\Delta T/\Delta x$$

The uncertainty in q_w because of the variation of the different terms is then given by the expression,

$$\delta q_w = q_w\,[(\delta k/k)^2 + (\delta T/T)^2 + (\delta x/x)^2]^{1/2}$$

where δk, δT and δx are uncertainties in thermal conductivity, measured boundary temperature and location of the measurement point, respectively. If a 10% uncertainty occurred in each of the terms, the uncertainty in heat flux would be 17.3%. The uncertainty due to variation in k alone is given by: $\delta q_w = \delta k$.

Similarly, the uncertainties in Q_w and R_w are expressed as:

$$\delta Q_w = Q_w\,[(\delta q_w/q_w)^2 + (\delta A/A)^2]^{1/2} = \delta q_w A, \text{ and}$$

$$\delta R_w = R_w\,[(\delta P_e/P_e)^2 + (\delta Q_w/Q_w)^2]^{1/2}$$

References

[1] Addepalli, S., Zhao, Y., Roy, R., Galhenege, W., Colle, M., Yu, J., Ucur, A. Non-destructive evaluation of localised heat damage occurring in carbon composites using thermography and thermal diffusivity measurement. Measurement 2019; 131:706–713.

[2] Delahaigue, J., Chatelain, J.-F., Lebrun, G. Influence of Cutting Temperature on the Tensile Strength of a Carbon Fiber-Reinforced Polymer. Fibers 2017; 5(4):46.

[3] Wang, H., Sun, J., Zhang, D., Guo, K., Li, J. The effect of cutting temperature in milling of carbon fiber reinforced polymer composites. Composites Part A 2016; 91:380–387.

[4] Mullier, G., Chatelain, J. F. Influence of Thermal Damage on the Mechanical Strength of Trimmed CFRP. Int. J. Mechanical and Mechatronics Eng. 2015; 9(8):1551–1558.

[5] Zitoune, R., Cadorin, N., Collombet, F., Šíma, M. Temperature and wear analysis in function of the cutting tool coating when drilling of composite structure: In situ measurement by optical fiber. Wear 2017; 376-377:1849-1858.

[6] Furuki, T., Hirogaki, T., Aoyama, E., Kodama, H., & Ogawa, K. Influence of Tool Shape and Coating Type on Machined Surface Quality in Face Milling of CFRP. Advanced Materials Research 2014; 1017:310–315.

[7] Kerrigan, K., O'Donnell, G. E. Temperature measurement in CFRP milling using a wireless tool-integrated process monitoring sensor. International Journal of Automation Technology 2013; 7(6):742–750.

[8] Merino-Perez, J. L., Royer, R., Ayvar-Soberanis, S., Merson, E., & Hodzic, A. On the temperatures developed in CFRP drilling using uncoated wc-co tools part I: Workpiece constituents, cutting speed and heat dissipation. Composite Structures 2015; 123:161–168.

[9] Yashiro, T., Ogawa, T., & Sasahara, H. Temperature measurement of cutting tool and machined surface layer in milling of CFRP. International Journal of Machine Tools and Manufacture 2013; 70:63-69.

[10] Liu, J., Chen, G., Ji, C., Qin, X., Li, H., Ren, C. An investigation of workpiece temperature variation of helical milling for carbon fiber reinforced plastics (CFRP). International Journal of Machine Tools and Manufacture 2014; 86:89–103.

[11] Sheikh-Ahmad, J. Y., Almaskari, F., Hafeez, F., Meng, F. Evaluation of heat partition in machining CFRP using inverse method. Machining Science and Technology 2019; 23(4):530-546.

[12] Woo, T. K., Ahmad, F., Sharif, S., Maoinser, M. A. Effects of Drilling Generated Heat on Damage Factor in GFRP. Key Engineering Materials 2013; 594–595:661–665.

[13] Mkaddem, A., Zain-ul-abdein, M., Mezlini, S., Mahfouz, A. S. Bin, Jarraya, A. Sensitivity of GFRP Composite Integrity to Machining-Induced Heat : A Numerical Approach. In: Fakhfakh T., Chaari F., Walha L., Abdennadher M., Abbes M., Haddar M. (eds) Advances in Acoustics and Vibration. Applied Condition Monitoring, 2017, vol 5. Springer, Cham

[14] Shaw, M.C. Metal Cutting Principles, 2nd Ed. Oxford University Press, Oxford, UK, 2005

[15] Ozisik, M.N. and Orlande, H.R.B. Inverse heat transfer fundamentals and applications 2000; Taylor & Francis, New York

[16] Kim, H-J, Kim, N-K, Kwak, J-S, Heat flux distribution model by sequential algorithm of inverse heat transfer for determining workpiece temperature in creep feed grinding. Int. J. Mach Tool Manuf. 2006; 46:2086-2093.

[17] Kalogiannakis, G., Van Hemelrijck, D., & Van Assche, G. Measurements of thermal properties of carbon/epoxy and glass/epoxy using modulated temperature differential scanning calorimetry. Journal of Composite Materials 2004; 38(2):163–175.

[18] Sölter, J., & Gulpak, M. Heat partitioning in dry milling of steel. CIRP Annals - Manufacturing Technology 2012; 61(1):87–90.

[19] Luchesi, V. M., & Coelho, R. T. An inverse method to estimate the moving heat source in machining process. Applied Thermal Engineering 2012; 45–46:64–78.

[20] Kerrigan, K., O'Donnell, G. On the Relationship between Cutting Temperature and Workpiece Polymer Degradation During CFRP Edge Trimming. Procedia CIRP 2016; 55: 170-175.

[21] Experimental Methods for Engineers, J.P. Holman, 7th edition, McGraw Hill, New York, 2001